CHEMICAL ENGINEERING TRANSACTIONS
VOL. 81, 2020
A publication of AIDIC
The Italian Association of Chemical Engineering
Online at www.cetjournal.it
Guest Editors: Petar S. Varbanov, Qiuwang Wang, Min Zeng, Panos Seferlis, Ting Ma, Jiří J. Klemeš

ISBN 978-88-95608-79-2; **ISSN** 2283-9216
DOI: 10.3303/CET2081219

Direct Pyrolysis Dehydrogenation Mechanism of Ammonia Borane and Alkali Metal Substituted Ammonia Borane

Suitao Qi*, Jiawei Yan, Libin Shi, Xiao Tan

Xian Jiaotong University, College of Chemical Engineering and Technology, 710049, Xian, Shaanxi, China
suitaoqi@mail.xjtu.edu.cn

As a material with high hydrogen storage density, ammonia borane has attracted the attention of researchers. Ammonia borane can release hydrogen gas through hydrolytic dehydrogenation and pyrolysis dehydrogenation, where hydrolytic dehydrogenation has a low actual hydrogen storage density and is expensive, which is not conducive to practical application. Direct thermal dehydrogenation research shows that improving the dehydrogenation performance of ammonia borane by metal substitution can not only increase the dehydrogenation rate, but also suppress the generation of impurity gases.
In this paper, the density functional theory (DFT) is used to calculate the structural parameters, density of states, and HOMO-LUMO energy difference to obtain the dehydrogenation stability of ammonia borane and alkali metal substituted ammonia borane. Subsequently, the reaction energy barriers of the N-H ... H-B path and the M-H ... H-N path are calculated to obtain which dehydrogenation path is easy to occur. The results show that alkali metal substituted ammonia borane MAB(M = Li, Na, K) is easier to dehydrogenate than AB, and MAB is more likely to dehydrogenate by forming M-H ... H-N double hydrogen bonds. Density functional theory calculations can obtain the structural parameters and related thermodynamic information of each stagnation point on the dehydrogenation reaction path, which provides theoretical guidance for the research and improvement of the dehydrogenation performance of ammonia borane.

1. Introduction

The development and utilization of hydrogen energy is restricted by its storage and transportation technology. Current common hydrogen storage materials include Microporous materials (Pan et al., 2004), alloy materials (Lee et al., 2020), liquid organic hydrogen storage materials (Verevkin et al., 2020) and complex hydride materials (Biniwale et al., 2008), etc. They have shortcomings such as low hydrogen storage density, catalysts poisoned, and generating impurity gases. Ammonia borane (NH_3BH_3, AB) has received widespread attention by researchers for its high-quality hydrogen storage density. Ammonia borane can be hydrolytically dehydrogenated and directly thermally dehydrogenated. The thermal decomposition reaction has disadvantages of high initial dehydrogenation temperature and slow dehydrogenation rate. The researchers found that (1) adding suitable accelerators or additives, such as Ni, Co nanoparticles (He et al., 2009), cobalt halide CoX_2 (Chiriac et al., 2011), divalent metal chloride MCl_2 (Toche et al., 2014), graphite carbon nitride C_3N_4 (Zhang et al., 2013) etc.; (2) Nano-domain effect, loading ammonia borane to mesoporous C materials such as CMK-3 (Hou et al., 2017), metal organic framework materials such as Ni (Gonzalez-Buch et al., 2013) or Co (Gao et al., 2013) modified MIL-101, JUC-32 (Li et al., 2010), MOF-74 (Gadipelli et al., 2011), ZIF-8 (Zhong et al., 2012); (3) Metal substitution method (Li (Xiong et al., 2008), Na, K (Wu et al., 2008), Ca (Luedtke et al. 2010), Sr, Al (Zhang et al., 2010), etc. to replace ammonia boron H atoms on N in the alkane) to improve the pyrolysis dehydrogenation performance of ammonia borane.
In this paper, the first principle of density functional theory (DFT) and molecular dynamics methods are used to calculate the possible reaction paths of AB and MAB (M = Li, Na, K). Providing theoretical guidance for ammonia borane and alkali metal ammonia borane directly thermally dehydrogenated.

Paper Received: 30/04/2020; Revised: 28/06/2020; Accepted: 30/06/2020
Please cite this article as: Qi S., Yan J., Shi L., Tan X., 2020, Direct Pyrolysis Dehydrogenation Mechanism of Ammonia Borane and Alkali Metal Substituted Ammonia Borane, Chemical Engineering Transactions, 81, 1309-1314 DOI:10.3303/CET2081219

2. Calculation method

The mechanism of pyrolysis and dehydrogenation of ammonia borane and metal ammonia borane was calculated using Gaussian 03. Using the B3LYP method in density functional theory DFT and the 6-311+G**(d, p) basis set to calculate the structure optimization and frequency of each reactant, transition state, intermediate and product in the reaction path, all optimizations are obtained Structural data of the structure (bond length, bond angle, dihedral angle, etc.), vibration frequency, zero point vibration energy (ZPE) and zero point energy correction, related thermodynamic analysis data (total energy, enthalpy, Gibbs free energy and related thermal correction. The transition state is searched by TS, QST2 or QST3 method.

3. Results and discussion

3.1 Structural parameters, density of states and HOMO-LUMO energy

The compound one H on the N atom in NH_3BH_3 is replaced by an alkali metal M (Li, Na, K) atom obtains MNH_2BH_3 (MAB). The optimized structure of AB and MAB after optimization under B3LYP/6-311+G**(d, p) is shown in Figure 1. After the introduction of M atoms, the two B-H bonds in MAB are also significantly longer than AB, and are easier to break away.

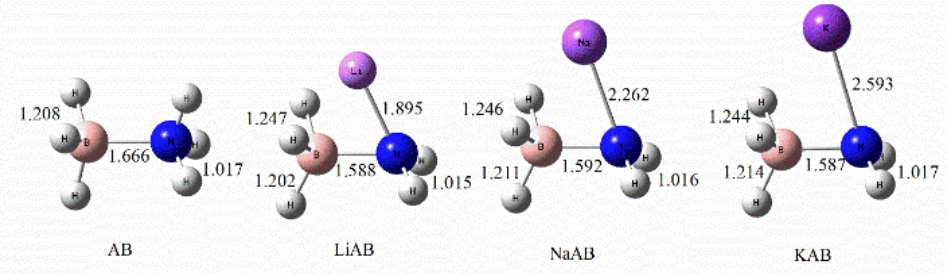

Figure 1: The geometric parameters of the most stable structure of AB and MAB (M = Li, Na, K) after optimization (bond length unit: Å). Note: Pink, blue, and white spheres represent B, N, and H atoms, and purple spheres are Li, Na, and K atoms from light to deep

The total state density and local state density of AB, MAB (M = Li, Na, K) are shown in Figure 2. According to calculations, they have a clear band gap between the valence band and the conduction band, showing the characteristics of the insulator. Their stability sequence is: KAB <NaAB <LiAB <AB, indicating that the electronic transition in MAB is easier than AB.

The highest occupied orbit (HOMO) and the lowest unoccupied orbit (LUMO) play an important role in the chemical properties of molecules. HOMO-LUMO energy level can be used to measure whether a molecule is easily excited. In this paper, the HOMO-LUMO energy levels of AB, LiAB, NaAB, and KAB are calculated to be 6.555, 5.50, 4.24, and 4.14 eV,. This value reflects the stability of AB and MAB, and the previously predicted stability (AB> LiAB> NaAB > KAB) Consistent. That is, introducing metal atom M to replace H on N in AB can reduce the initial dehydrogenation temperature of AB, that is, MAB is easier to dehydrogenate than AB.

3.2 Pyrolysis dehydrogenation mechanism of ammonia borane and alkali metal ammonia borane

3.2.1 Pyrolysis dehydrogenation of NH_3BH_3

Ammonia borane pyrolysis dehydrogenation only considers the first two steps of dehydrogenation. Ammonia borane forms N-H...H-B bond dehydrogenation by proton hydrogen at NH_3 end and negatively charged hydrogen at BH_3 end in the molecule. In this paper, the basic structural characteristics and potential energy of the relevant reactants, transition states and products dehydrogenation processes of AB in the gas phase are calculated. The dehydrogenation reaction process are shown in Figure 3, the reaction potential energy surface is shown in Figure 4. The energy barrier of the second dehydrogenation is greater, which is its control step. In addition, according to the structural optimization, NHBH(FS2), the product after the second step of dehydrogenation is linear. The two H's are located at both ends of the molecule, with A distance of 3.396 Å, indicating that they form N-H...B-H double hydrogen bonding is very difficult to continue dehydrogenation.

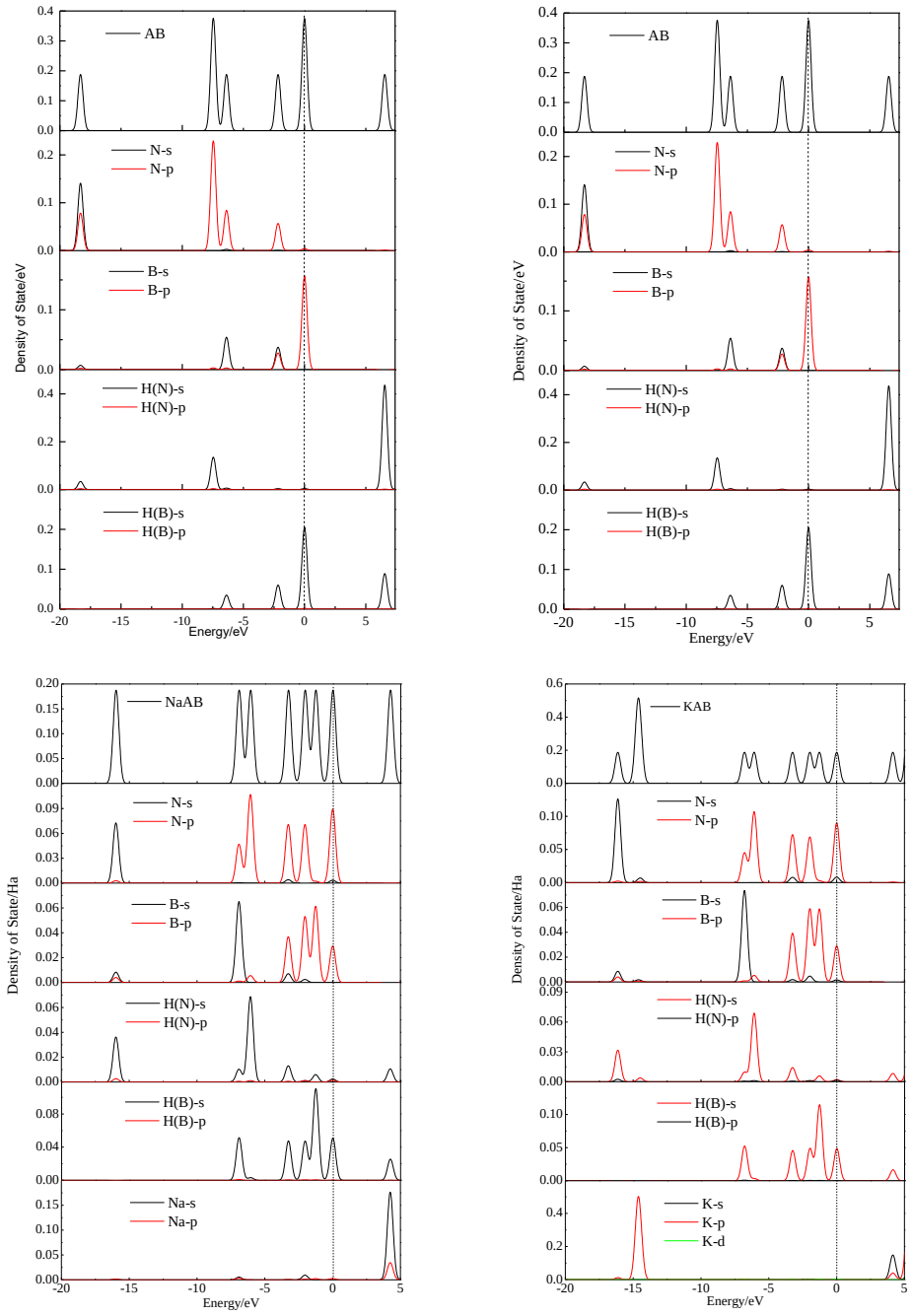

Figure 2: AB, MAB (M = Li, Na, K) total state density and local state density diagram

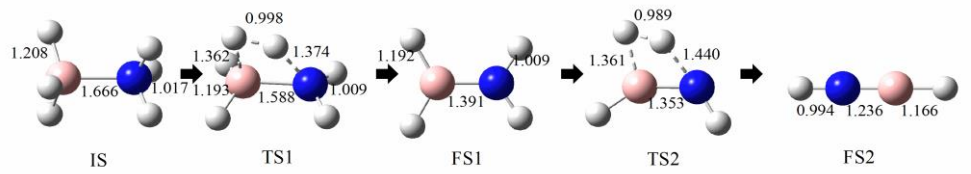

Figure 3: Schematic diagram of ammonia borane pyrolysis dehydrogenation process and the molecular structure of the reactants, transition states and products at various steps. (Note: IS, TS and FS represent the initial reactants, transition states and products, bond length unit: Å)

3.2.2 Synthesis of MNH_2BH_3 (M = Li, Na, K)

MNH_2BH_3 can be prepared by ball milling (or reacting in a solvent THF) of alkali metal hydrides MH (LiH, NaH, KH) and NH_3BH_3. The potential energy is shown in Figure 5.

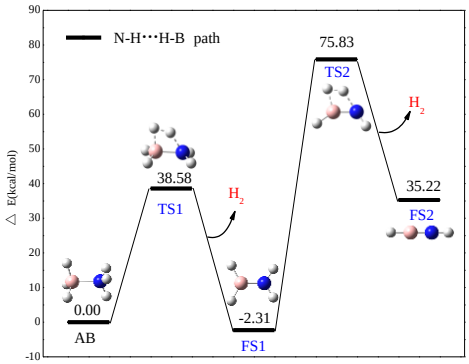

Figure 4: Potential energy surface diagram of the stepwise reaction of NH_3BH_3 pyrolysis dehydrogenation (N-H ... H-B path)

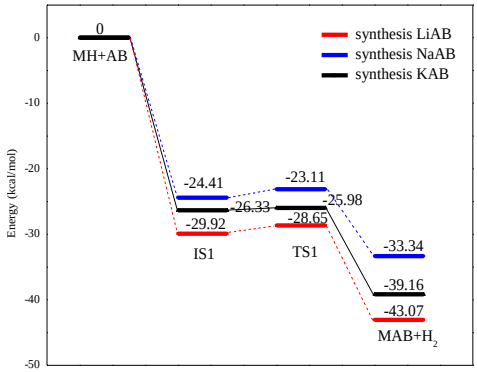

Figure 5: Potential energy surface diagram of the preparation of MNH_2BH_3 by the reaction of MH and NH_3BH_3

According to calculations, the energy barriers of LiAB, NaAB, and KAB prepared by the reaction of LiH, NaH, KH, and NH_3BH_3 (1.27, 0.7, and 0.35 kcal/mol) indicate that the reaction is easier to proceed.

3.2.3 MNH_2BH_3 (M = Li, Na, K) pyrolysis dehydrogenation mechanism

The pyrolysis and dehydrogenation of MNH_2BH_3 are carried out step by step. The reaction steps are shown in the following reaction formula:

$MNH_2BH_3 \rightarrow MNHBH_2+H_2$ (1)

$MNHBH_2 \rightarrow MNBH+H_2$ (2)

In this paper, two possible mechanisms for pyrolysis and dehydrogenation of MNH_2BH_3 in the gas phase are calculated: (a) the formation of N-H ... H-B double hydrogen bond dehydrogenation; (b) the generation of M-H, which is dehydrogenated by M-H ... H-N double hydrogen bond.

(1) N-H ... H-B dehydrogenation path

The first step of dehydrogenation is from the initial state IS (MNH_2BH_3, MAB) of the reactant via the transition state TS1 to the first step dehydrogenation product FS1 ($MNHBH_2$). The second step dehydrogenation from FS1 ($MNHBH_2$) via the transition state TS2 to the second step dehydrogenation product FS2 (MNBH). In the process of dehydrogenation of MAB through N-H ... H-B double hydrogen bond, the energy barrier of the second dehydrogenation is the largest, which is the control step of this reaction.

The energy barrier of MAB dehydrogenation by N-H ... H-B is similar to AB, and the initial temperature of MAB dehydrogenation is lower than that of AB, so it is speculated that MAB is unlikely to be dehydrogenated by N-H…H-B.

(2) M-H ... H-N dehydrogenation path

The key to the thermal dehydrogenation of MAB through path (b) M-H ... H-N is to form M-H, and then M-H and N-H at the NH_2 terminal form a double hydrogen bond M-H ... H-N to further dehydrogenate. The first step of

dehydrogenation is from the initial state of the reactant IS1 (MNH_2BH_3, MAB) via the transition state TS1-1 to the intermediate IM1, and then from the intermediate IM1 via TS1-2 to the first step dehydrogenation product FS1 ($MNHBH_2$). Next, a second dehydrogenation occurs, from the first dehydrogenation product FS1 ($MNHBH_2$) via the transition state TS2-1 to the intermediate IM2, and finally from the intermediate IM2 via the transition state TS2-2 to the second step dehydrogenation product FS2 (MNBH).

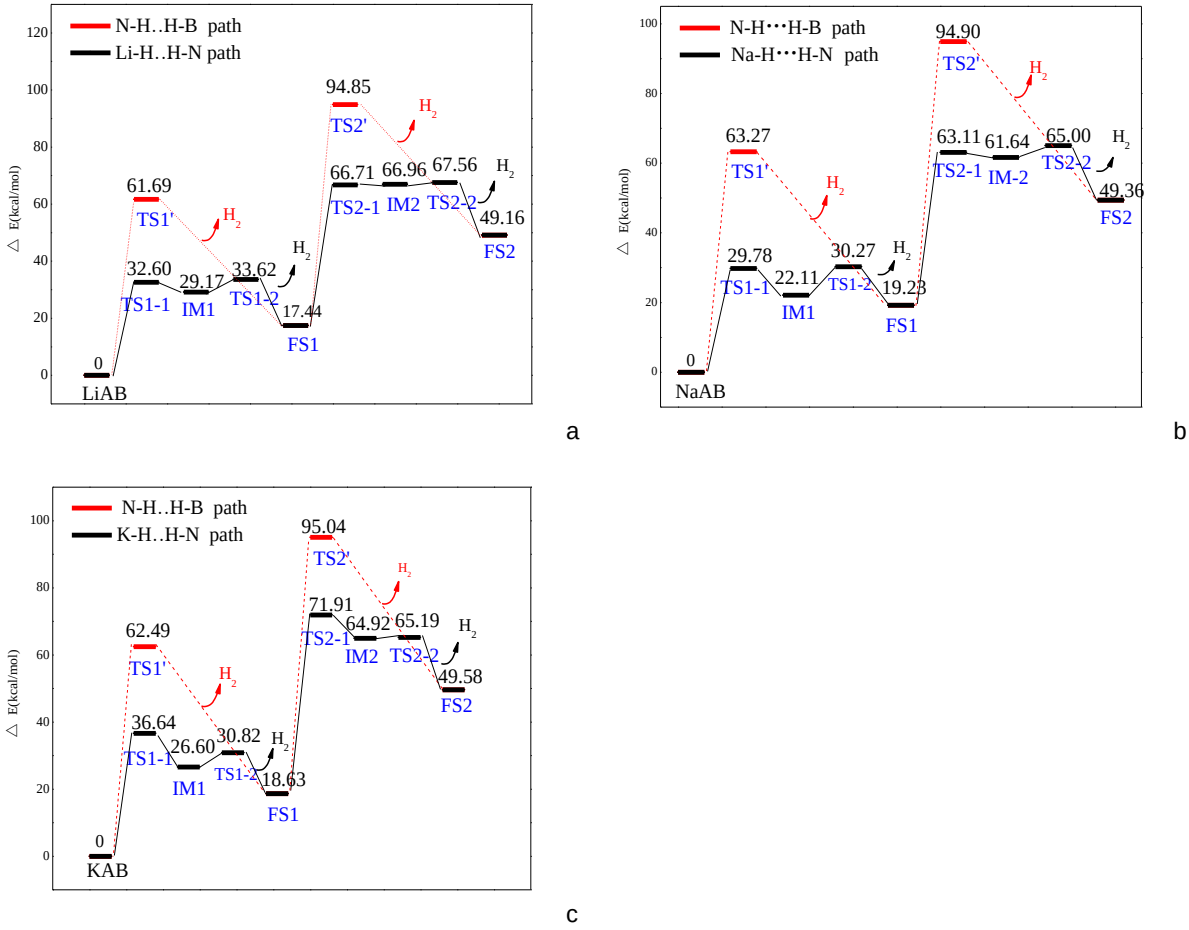

Figure 6: Potential energy surface of MNH_2BH_3 (M = Li, Na, K) through the path (1) N-H ... H-B or (2) M-H ... H-N pyrolysis dehydrogenation stepwise reaction

(3) Comparison of two pyrolysis dehydrogenation paths of MAB

Table 1: Comparison of energy barriers for AB and MAB stepwise dehydrogenation through different paths

Energy barrier / MAB	First step dehydrogenation(kcal·mol^{-1})		Second step dehydrogenation(kcal·mol^{-1})	
	N-H…H-B Path	M-H…H-N Path	N-H…H-B Path	M-H…H-N Path
AB	38.58	/	78.14	/
LiAB	61.69	32.60	77.41	49.27
NaAB	63.27	29.78	75.67	43.88
KAB	62.49	36.64	76.41	53.28

Comparing the two dehydrogenation paths of MAB, in the two-step dehydrogenation process, the energy barriers of LiAB, NaAB, and KAB dehydrogenation through the M-H ... H-N path are significantly smaller than the N-H ... H-B path. The energy barriers of LiAB, NaAB and KAB through the M-H ... H-N two-step dehydrogenation are less than AB. The first-step dehydrogenation energy barrier reflects the initial dehydrogenation temperature of MAB; the second-step dehydrogenation is the reaction control step. It shows that MAB can significantly increase the dehydrogenation rate than AB. In summary, MAB decomposes the main reaction path by pyrolysis dehydrogenation through the path of forming M-H ... H-N double hydrogen bonds.

4. Conclusions

Using density functional theory (DFT) in B3LYP/6-311+G**(d, p) to calculate the ammonia borane (AB) and alkali metal ammonia borane (MAB, M = Li, Na, K) pyrolysis dehydrogenation reaction in the gas phase, theoretical calculation results show that:

(1) According to molecular structure, density of states, and HOMO-LUMO energy level difference analysis, the stability of AB, LiAB, NaAB, and KAB decreases in turn, indicating that the stability and the initial dehydrogenation temperature is reduced.

(2) MAB can be prepared by ball milling (or reacting in THF) of MH and NH_3BH_3. The energy barrier of this reaction is very small (about 1 kcal · mol^{-1}), indicating that the reaction is easy to occur.

(3) For the MAB pyrolysis dehydrogenation reaction, the energy barrier for dehydrogenation by forming MH ... HN double hydrogen bonds is much lower than that for NH ... HB double hydrogen bonds, indicating that MAB is more likely to form MH … HN double hydrogen bond dehydrogenation. The energy barrier for dehydrogenation by M-H ... H-N double hydrogen bond is smaller than that for AB dehydrogenation, indicating that MAB is easier to dehydrogenate than AB. In the M-H ... H-N path, it is found that the MAB dehydrogenation reaction rate sequence is: KAB < LiAB < NaAB.

References

Pan L., Sander M.B., Huang X., Li J., Smith M., Bittner E., 2004, Microporous metal organic materials: promising candidates as sorbents for hydrogen storage, Journal of the American Chemical Society, 126(5), 1308-1309.

Lee J., Park C., Park H., Kang N., 2020. Effective hydrogen diffusion coefficient for cocrfemnni high-entropy alloy and microstructural behaviors after hydrogen permeation, Int J of Hydrogen Energy, 45(16).

Verevkin S.P., Pimerzin A.A., Sun L.X., 2020, Liquid organic hydrogen carriers: Hydrogen storage by di-phenyl ether derivatives: An experimental and theoretical study, The Journal of Chemical Thermodynamics, 144, 106057.

Biniwale R.B., Rayalu S., Devotta S., 2008, Chemical hydrides: A solution to high capacity hy-drogen storage and supply, International Journal of Hydrogen Energy, 33(1), 360-365.

He T., Xiong Z., Wu G., 2009, Nanosized Co- and Ni-catalyzed ammonia borane for hydrogen storage, Chemistry of Materials, 21, 2315-2318.

Chiriac R., Toche F., Demirci U.B., 2011, Ammonia borane decomposition in the presence of cobalt halides, Fuel & Energy Abstracts, 36(36), 12955-12964.

Toche F., Chiriac R., Demirci U.B., 2014, Ammonia borane thermolytic decomposition in the presence of metal (II) chlorides, International Journal of Hydrogen Energy, 12(10), 651-669.

Zhang J., He T., Liu L., 2013, Effects of graphitic carbon nitride on the dehydrogenation of ammonia borane, Chinese Journal of Catalysis, 34, 1303-1311.

Hou C., Li Q., Wang C., Peng C., Chen Q., Ye H., 2017, Ternary Ni–Co–P nanoparticles as noble-metal-free catalysts to boost the hydrolytic dehydrogenation of ammonia-borane, Energy & Environmental Science, 10(8), 1770-1776.

Gonzalez-Buch C., Herraiz-Cardona I., Ortega E.M., Garcia-Anton J., Perez-Herranz V., 2013, Development of Ni-Mo, Ni-W and Ni-Co macroporous materials for hydrogen evolution reaction, Chemical Engineering Transactions, 32, 865-870.

Gao L., Li C.Y.V., Yung H., 2013, A functionalized MIL-101 (Cr) metal–organic framework for enhanced hydrogen release from ammonia borane at low temperature, Chemical Communications, 49(90), 10629-10631.

Li Z., Zhu G., Lu G., 2010, Ammonia borane confined by a metal- organic framework for chemical hydrogen storage: enhancing kinetics and eliminating ammonia, Journal of the American Chemical Society, 132(5), 1490-1491.

Gadipelli S., Ford J., Zhou W., 2012, Nanoconfinement and Catalytic Dehydrogenation of Ammonia Borane by Magnesium-Metal-Organic-Framework-74, Chemistry-A European Journal, 17(22), 6043-6047.

Zhong R.Q., Zou R.Q., Nakagawa T., 2012, Improved Hydrogen Release from Ammonia–Borane with ZIF-8, Inorganic Chemistry, 51(5), 2728-2730.

Xiong Z., Wu G., Chua Y.S., Hu J., He T., Xu W., 2008, Synthesis of sodium amidoborane ($NaNH_2BH_3$) for hydrogen production, Energy & Environmental Science, 1(3), 360-363.

Wu H., Zhou W., Yildirim T., 2008, Alkali and alkaline-earth metal amidoboranes: structure, crystal chemistry, and hydrogen storage properties, Journal of the American Chemical Society,130(44), 14834-14839.

Luedtke A.T., Autrey T., 2010, Hydrogen release studies of alkali metal amidoboranes, Inorganic Chemistry, 49(8), 3905-3910.

Zhang Q., Tang C., Fang C., 2010, Synthesis, crystal structure, and thermal decomposition of strontium amidoborane, The Journal of Physical Chemistry C, 114(3), 1709-1714.